Pergamon

Phys. Chem. Earth, Vol. 23, No. 9–10, pp. 1053–1068, 1998

0079-1946/98/$—see front matter

PII: S0079-1946(98)00145-1

Observations of the Earth's Topography from the Shuttle Laser Altimeter (SLA): Laser-pulse Echo-recovery Measurements of Terrestrial Surfaces

J. Garvin[1], J. Bufton[1], J. Blair[1], D. Harding[1], S. Luthcke[2], J. Frawley[2] and D. Rowlands[1]

[1]Laboratory for Terrestrial Physics, NASA Goddard Space Flight Center (GSFC), Greenbelt, MD 20771, U.S.A.
[2]Raytheon STX at NASA GSFC

Received 25 October 1997; accepted 24 April 1998

Abstract. Meter-precision topographic measurements of a diverse suite of terrestrial surfaces have been accomplished from Earth orbit using the Shuttle Laser Altimeter (SLA) instrument flown aboard the Space Shuttle *Endeavour* in January of 1996. Over three million laser pulses were directed at the Earth by the SLA system during its ~ 80 hours of nadir-pointing operation at an orbital altitude of 305 km (+/- 10 km). Approximately 90% of these pulses resulted in valid range measurements to ocean, land, and cloud features. Of those which were fired at land targets, 57% resulted in valid surface ranges, the remainder being cloud tops, false alarms, or missed shots. The SLA incorporated an electronic echo-recovery system into a pulsed, time-of-flight laser altimeter instrument in order to capture and characterize the vertical structure within each 100 m diameter surface footprint. The echoes recorded by SLA demonstrate aspects of the vertical structure of the nearly ubiquitous vegetation cover on the planet, as well as sensitivity to local slopes, surface reflectivity, and vertical ruggedness. With a vertical resolution of 0.75 m and horizontal sampling at 0.7 km length scales, SLA provides a new form of high vertical accuracy topographic data for studying problems related to the dynamics of the Earth's surface. Assessment of the error budget associated with the SLA experiment suggests that ~2.8 m (RMS) precision was achieved for ranging measurements to oceanic surfaces, for which there are over 700,000 examples. With the availability of a precision radial orbit and post-flight Shuttleattitude information, a mid-latitude (+ 28.5° to -28.5°), georeferenced database of topographic ground control point elevations has been achieved using SLA data, consisting of ~ 344,000 land measurements. Each of these measurements is geolocated to within 1-2 SLA footprints (100-200 m) on the Earth's surface, with vertical errors that approach the limits of resolution (0.75 m) of the instrument in topographically benign regions. When compared to available Digital Elevation Models (DEM's) with stated vertical accuracies on the order of 10-16 m, SLA's measurements differ by no more than 11 m to 46 m RMS in rugged terrain. We have computed a total vertical roughness parameter for all multi-peaked SLA echoes using a multi-Gaussian decomposition technique and have observed a very high degree of correlation of this parameter with global landcover classes. In some cases (~6%), SLA echoes clearly resolve both the ground surface and vegetation canopy within a single footprint, suggesting that the modal height of equatorial vegetation is ~ 18 m. The global distribution of total vertical roughness varies from ~ 5 m to 60 m, with a mean value of 27 m and a standard deviation of 12 m. SLA successfully served as a pathfinder for high vertical resolution orbital topographic remote sensing instrumentation, and demonstrated the first high resolution echo-recovery laser altimeter observations over land surfaces.

Correspondence to:

Dr. J. B. Garvin
Code 921, Geodynamics, Bldg. 22, Room 132
NASA Goddard Space Flight Center
Greenbelt, MD 20771 USA
TEL: 301-286-6565
FAX: 301-286-1616
Email: garvin@denali.gsfc.nasa.gov

1. Introduction

Direct measurements of the topography and vertical structure of the surface of the Earth from a spaceborne perspective are in their infancy, and to date, only limited real-aperture radar altimeter (RAR) instruments (Zwally et al., 1983; Bindschadler et al., 1989; Wingham et al., 1994) have acquired observations over both land and ocean surfaces. More traditional stereogrammetric methods (Burke and Dixon, 1988; Harding et al., 1994a), as well as interferometric synthetic aperture radar (ISAR) techniques (Evans et al., 1992; Zebker et al., 1992; Madsen et al., 1993; Zebker et al., 1994), can produce digital elevation model (DEM) datasets using pairs of spaceborne images, but such approaches require independent, ground control point information to produce reliable results at vertical accuracies of 10 m or better. One of the emerging scientific themes in global Earth System Science involves measurement of seasonal to interannual Earth surface changes, and hence requires an initial reference framework or baseline; the Earth's land, ocean and ice topography is an often-mentioned example (Burke and Dixon, 1988; TOPSAT Working Group, 1994). Thus, direct measurement of global topography in a suitable Earth center-of-mass reference frame and with appropriate vertical accuracy and horizontal sampling has been a frustratingly unattainable objective for many problems within the context of the U. S. Global Change Research Program (USGCRP). Laser-based (i.e., active optical) techniques have been under development that offer complementary capabilities to microwave-based approaches such as ISAR and RAR. This article addresses the first Earth orbital application of laser technology for the purpose of high precision land topography remote sensing.

There exists a subset of scientific problems in global Earth Systems Science that require extremely high vertical accuracy topographic data, as well as sensitivity to the distribution of vertical structure within each measurement footprint on the Earth's surface. For example, in areas of extremely mundane relief, such as is found in many coastal regions, remote sensing measurements of meter-level subtleties of local relief at kilometer length scales are needed in order to assess patterns and rates of erosion or accretion. Existing knowledge of the 1-10 km scale topography of many of the Earth's largest river delta systems, for example, is limited to 100 m vertical precision datasets derived from stereogrammetric contour maps (Coleman and Wright, 1975; Wright, 1985; Coleman et al., 1989). In the so-called featureless regions of the great deserts of the Earth, local relief may vary by only a few tens of meters across 100's of kilometers, and measurement of the time-varying nature of this ephemeral relief is important in the context of global models of climate change and for desertification studies (Lancaster, 1995). The existing global database of land topography, however, is known to be woefully inadequate for studies of many coastal and desert regions (Loughridge, 1986; Burke and Dixon, 1988).

Other issues associated with topographic remote sensing of terrestrial surfaces concern observations of the ground topography in the presence of vegetation cover. Aside from the hyperarid deserts and a narrow strip of coastal landforms, most of the land surface of Earth (i.e., ~ 85%) is covered with some form of vegetation, ranging from continuous grass cover to nearly closed canopy woody plants (i.e., trees) (Harding et al., 1994a). How to measure the ground topography under the trees remains a fundamental problem, especially if the objective is to accomplish such measurements from a spaceborne perspective (Burke and Dixon, 1988). While ISAR methods show great promise for high spatial resolution topographic mapping of the Earth's land surfaces (Evans et al., 1992; Mouginis-Mark and Garbeil, 1993), it remains unclear how well ISAR measurements can provide reliable topographic data for sub-canopy ground surfaces. This is because microwave penetration of vegetation canopies is dependent upon the water content of the canopy materials and may vary as a function of location and biome (Evans et al., 1992; Zebker et al., 1992; Madsen et al., 1993; Zebker et al., 1994). Many regions with active or potentially active volcanoes would benefit from topographic observations of the highly vegetated unstable flanks of these dynamic edifices, yet most existing topographic maps for such features display large vertical uncertainties in regions with extensive vegetation (Mouginis-Mark and Garbeil, 1993; Garvin, 1996). In addition, measurement of the relative relief of the vegetation cover offers the means to address an important problem (i.e. landscape aerodynamic roughness), especially as it relates to global climate models and short-term climate variability (Harding et al., 1994b; Blair et al., 1994). Direct assessment of vegetation heights from a spaceborne perspective would facilitate improved model predictions of global ecosystems behavior and biomass.

Finally, direct observation of the relative and absolute relief of the most rugged mountainous regions of the planet, including the Himalayan frontal ranges and the high Andes, are important goals in the context of geomorphological studies of Earth. The human inaccessibility of such places makes precision observations of their quantitative relief characteristics difficult to attain, and snow and ice cover often make traditional stereogrammetric methods subject to significant inaccuracies (Burke and Dixon, 1988; Harding et al., 1994a). There are documented mountain systems in both Africa and South America where the vertical precision of the best available topographic data is on the order of 1000 m, averaged on a ~ 10 km length scale (Burke and Dixon, 1988). This is inadequate for any hydrologic studies, and improved measurements are clearly needed (Burke and Dixon, 1988; TOPSAT Working Group, 1994).

Airborne laser altimeter sensors have been in operation since the late 1980's for the purpose of scientific studies of land and ice surfaces (Bufton, 1989; Bufton et al., 1991; Garvin, 1993; Blair et al., 1994; Krabill et al., 1995a; Krabill et al., 1995b; Garvin, 1996). Recent improvements in airborne systems have culminated in a suite of experimental sensors, including relatively wide-swath echo-recovery instruments and low-altitude scanning lidar terrain mapping systems (Blair et al., 1994; Krabill et al., 1995a; Krabill et al., 1995b; Garvin, 1997). Routine airborne topographic monitoring of volcanoes, ice sheets, glaciers,

coastal landforms, tectonized landscapes, ecosystems, and other phenomena is an ongoing element of NASA's Office of Earth Science (OES) Program. Examples of results in some of these subdisciplines can be found in various published articles, including those by Bufton (1989), Bufton et al., (1991), Garvin (1993; 1996; 1997), Harding et al. (1994a; 1994b), Blair et al. (1994), and Krabill et al. (1995a; 1995b). While airborne laser altimeter systems offer regional access to important scientific problems at extremely high spatial and vertical resolution, global access within a common, Earth center-of-mass reference frame is required to address many critical Earth System Science problems. Global sampling via orbital laser altimetry has been achieved, for the first time, with the Shuttle Laser Altimeter.

2. Spaceborne laser altimetry

Laser altimeter instruments have operated in the space environment to a very limited extent before 1996. Simple, yet elegant ruby laser altimeter systems were flown aboard the Apollo 15, 16, and 17 Command Service Module spacecraft in lunar orbit in order to provide occassional ground control points from which to calibrate metric stereo photographs (Garvin, 1993; Zuber et al., 1994; Smith et al., 1997). These low pulse repetition rate devices recorded a few thousand measurements of the topography of the lunar surface in a geodetic coordinate frame from which an assessment of the center of mass versus center of figure offset was successfully performed.

Various Soviet Earth-orbiting spacecraft in the 1980's carried limited light detection and ranging (lidar) instruments that made measurements of the range to the Earth's surface at modest pulse repetition rates (i.e., 1 Hz). The electronics associated with these spaceborne lidar instruments were primarily designed to analyze atmospheric phenomena such as clouds and were not optimized for high pulse repetition rate ground ranging measurements (Matvienko et al., 1994; Balin et al., 1994; Matvienko et al., 1995). The U.S. Space Shuttle flight of the LITE experiment in September of 1994 on STS-64 also provided a set of lidar observations from Earth orbit (Winker et al., 1996). The Laser-in Space Technology Experiment (LITE) was designed to measure atmospheric phenomena, including boundary layer aerosols and clouds, and in addition, accomplished successful measurements to terrestrial ocean and land surfaces, albeit at low (>25 m) vertical resolution (Winker et al., 1996).

The U.S. Clementine spaceborne LIDAR experiment included a laser rangefinding sensor that successfully measured the distance to the lunar surface from ranges as great as 640 km during the 1994 lunar orbital phase of the Clementine mission (Zuber et al., 1994). This compact device acquired measurements with 40 m vertical resolution once every 10-20 km along the nadir ground-track of the spacecraft. Data were acquired during a two month lunar operational period in early 1994, and approximately 70,000 "valid" topographic measurements were achieved, which corresponds to a ~ 20% measurement success rate (Smith et al., 1997). In spite of this small instrument's extreme sensitivity to the ruggedness of the lunar surface, the geodetic quality of the observations, when available, has provided scientifically compelling information regarding the longer wavelength (i.e., > 100 km) geophysics of the Moon (Zuber et al., 1994; Smith et al., 1997).

The Mars Observer Laser Altimeter (MOLA-1) sensor was originally designed in 1988-1990, and launched to Mars in late 1992 on the U. S. Mars Observer spacecraft. This instrument was intended for long-term, autonomous operation in a deep-space environment, and incorporated all solid-state laser transmitter technology with a receiver electronics package capable of "tracking" the most rugged (at 100 m length scales) landscapes imaginable (Zuber et al., 1992). Although MOLA-1 was lost in 1993 when the Mars Observer spacecraft failed to regain radio contact with Earth after its orbital insertion manoever, the instrument has been rebuilt (MOLA-2) with improved ranging resolution (i.e., < 0.5 m), and is presently in orbit around Mars as part of the U. S. Mars Global Surveyor mission. MOLA-2 will commence its global topographic mapping of Mars in early 1999, and is expected to produce a dataset consisting of nearly one billion measurements during its nominal 687-day mission. Initial examples of MOLA-2 data acquired as part of calibration activities indicate sub-meter-quality ranging precision (i.e., NASA Mars Global Surveyor Press Conference, Oct. 1997 and (Zuber et al., 1992)).

The development of the MOLA-class laser altimeter sensors served as a pathfinder for the Shuttle Laser Altimeter (SLA) in a variety of ways. SLA was able to capitalize on the MOLA-1 design and development experience, to assemble a spaceworthy 10 Hz laser transmitter out of MOLA-1 spare components, and to embellish the original MOLA design by including a waveform analyzer and larger capacity flight data system (Bufton et al., 1996). By utilizing spare components from the MOLA-1 sensor, the SLA instrument was developed at very low cost. Furthermore, SLA was deployed as a Hitchhiker experiment aboard an Earth-viewing Space Shuttle flight in order to maintain a low cost interface to the Shuttle while obtaining the required power, command, and telemetry services.

3. Objectives

The underlying objectives of the SLA-01 experiment were essentially two-fold: (1) to serve as an engineering pathfinder for high-resolution orbital laser altimeter observations of terrestrial surfaces; and (2) to provide pathfinding scientific datasets of value in addressing global Earth System science problems, and in particular those pertaining to land cover dynamics in arid and coastal areas, as well as in heavily vegetated regions. To fulfill the science and engineering objectives associated with the first Earth orbital flight of a high vertical resolution laser altimeter instrument, the core SLA sensor as derived from MOLA-1 spares was embellished to include a high

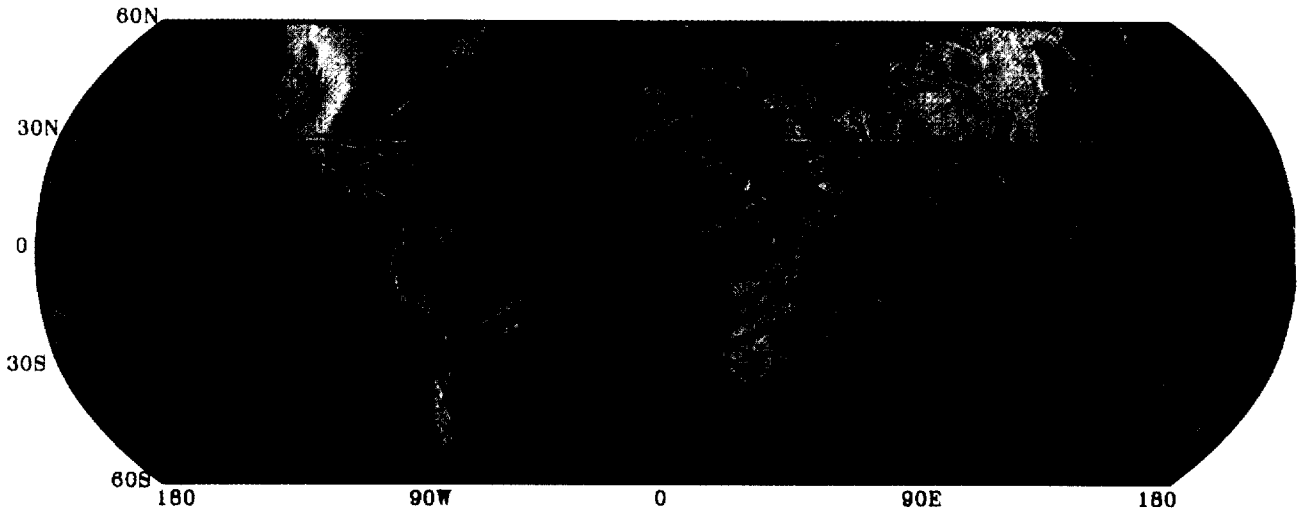

Fig. 1. SLA Earth Surface Coverage Map (all ground tracks obtained).

temporal resolution echo recovery system in order to digitize the amplitude versus time history of each backscattered laser pulse (Zuber et al., 1994; Bufton et al., 1996).

The SLA instrument was successfully first flown in Earth orbit between 11 and 20 January, 1996 aboard the U. S. Space Shuttle *Endeavour*, as part of the STS-72 mission (Garvin et al., 1996a; 1996b). Approximately 82 hours of data were acquired in a nadir-viewing orientation from the *Endeavour* orbiter. Due to the orbit inclination requirements of the STS-72 mission, only that region of the Earth between 28.45° N and 28.45° S latitudes was observed with SLA. Hence, the initial SLA dataset is restricted to mid-latitude studies of Earth surface (i.e., land and oceans) phenomena (Fig. 1).

As SLA was designed as a flexible, modular engineering pathfinder for heretofore unattainable observations, the scientific objectives were intentionally specified in broad terms. Among the more important goals were for SLA to demonstrate a high pulse repetition rate (i.e., 10 Hz), adequate signal to noise laser altimeter system capable of reliably ranging off of virtually all types of Earth surface targets and some varieties of optically opaque atmospheric phenomena (i.e., clouds). It has required nearly a year to completely calibrate and geolocate the majority of the ~ 3 million observations recorded by the SLA sensor while in Earth orbit, and to assess their validity. Examination of the data quality indicates robust ranging off of steep escarpments, tropical forest canopies, lava-covered summits of major volcanoes, stony-pavement deserts, snow-clad 6800 m mountains, and even complex urbanized surfaces (i.e., buildings in cities). A broad variety of cloud-top ranges were also recorded, including those associated with optically opaque features located less than 1000 m above the ocean surface.

The remainder of this article briefly describes the SLA instrumentation, outlines the data acquired during the January 1996 mission, and provides a series of examples to highlight the preliminary scientific findings of this experiment.

4. Laser altimeter techniques

The SLA instrument essentially consists of three major components: (1) an all-solid-state, diode pumped, Q-switched, Nd:YAG laser transmitter capable of continuously operating at up to 10 pulses per second; (2) an altimeter receiver electronics package in which the round-trip travel time of each individual laser pulse is measured at 5 nsec resolution using a time-interval unit (TIU): (3) a 250 Megasample/sec waveform recorder which digitizes each received pulse into a record of one hundred 8-bit samples, and a Cassegrain telescope 38 cm in diameter with a Silicon Avalanche Photo-Diode (Si APD) detector at the prime focus. A 386SX flight computer and associated data storage media are also essential sub-systems, as were power inversion electronics and temperature sensors. All of SLA'sdata was recorded directly on one of two 270 Megabyte hard disk drives, and during specific periods of high bandwidth communications with the Space Shuttle *Endeavour* from Earth using Ku-band links, data were transmitted to the SLA Payload Operations Control Center at NASA's Goddard Space Flight Center. Approximately 20% of the total SLA dataset was transmitted in real-time to the Earth for analysis by the engineering and science teams during the flight mission.

SLA was configured in two Hitchhiker Canisters arranged side-by-side on a bridge assembly that was mounted across the aft part of the Shuttle Orbiter cargo bay. This arrangement allowed the SLA sensor to be operated as a Hitchhiker experiment. Further details of the SLA configuration can be found in Bufton et al. (Bufton et al., 1996). Under command from the flight computer, the laser

transmitter is instructed to emit a short ~ 8 nsec full-width at half maximum (FWHM) pulse of 1064 nm radiation at the Earth's surface whose divergence (0.35 mrad) corresponds to a surface footprint of ~ 100 m from a 300 km orbital altitude. As the laser pulse is transmitted, a "start" pulse is generated which activates a high temporal resolution digital counter whose least significant bit of 5 ns duration corresponds to 0.75 m in range. The laser pulse intercepts either the Earth's surface or is backscattered by a cloud, causing a number of photons to be scattered back to the SLA telescope in the Space Shuttle where they are focused by the telescope's primary mirror onto the Silicon Avalanche PhotoDiode (Si APD) detector. If the backscattered signal is above the noise threshold, it generates a "stop" pulse to interrupt the digital counter and record the round trip travel time in discrete units of 5 ns. In the meantime, the successful detection of a backscattered pulse also starts the 250 Megasample per second waveform digitizer, which proceeds to record 100 discrete channels of pulse amplitude data as an electronic version of the echo received, with a total dynamic range of 60m. The digitized echo, together with the TIU round-trip travel time and time epoch information are then recorded by the flight computer on one of the ruggedized, internal hard disk drives. Operator control of the 37 parameters that can influence detection of valid ranges with the SLA instrument is possible during those times when low-rate radio communication (S-band) with the Shuttle Orbiter is enabled. The range gate delay and width can be set by two of these parameter update commands. For most of the SLA observation periods, the range gate width was set at 40 km. This was selected in order to account for the typically 10 km variations in the radial orbit of the Shuttle (i.e., ~ 300 to 310 km) in combination with the greatest relief relative to mean sea-level observed on Earth (8.85 km at Mount Everest), while rejecting noise outside of this interval.

Ancillary data pertaining to the position and attitude of the Space Shuttle *Endeavour* is essential if one is to accurately geolocate SLA's observations on the surface of the Earth and in the proper center-of-mass coordinate frame. Radial orbit data and roll, pitch, and yaw angles are available in the Shuttle telemetry stream and from other sources, and we have computed precision orbits and pointing angle corrections to facilitate highly accurate surface geolocation of the majority of SLA footprints. During part of the SLA observation sequence, the *Endeavour* orbiter was flown so as to maintain a nadir-orientation to within +/- 0.1° per axis (i.e., a 0.1° pointing control deadband). Even with this level of pointing control, a 0.1° offset in the pointing of SLA results in ~ 700 m of positional offset on the surface of the Earth relative to the nadir ground-track of the Shuttle. Most SLA data were acquired with a +/- 1.0° per axis pointing control deadband, which produces up to ~ 7 km of surface offset. These surface offsets are not uncertainties and have been accounted for using Shuttle-provided measurements of 3-axis attitude which have a stated precision of 0.03°. The vertical precision of the SLA surface elevation data is 1 - 10 m as a function of local slopes and landcover vertical structure, with a typical horizontal sampling interval of ~ 700 m, which is determined on the basis of the spacecraft platform orbital velocity (~7 km/s) and pulse repetition rate of the laser transmitter (10 Hz). The quality of the preliminary radial orbit for the Shuttle is on the order of 1 km spatially and ~ 0.1 km in a vertical sense (Rowlands et al., 1997). Precision orbit determination using GPS and TOPEX-TDRS-Shuttle tracking information has achieved ~ 1.5 m vertical (radial) orbits and < 150 m horizontal positioning (Rowlands et al., 1997).

The value of high-resolution altimetric data is only as good as the definition of the reference frame in which it is measured. For satellite altimetry in general, the position and orientation of the satellite platform (i.e., the Space Shuttle *Endeavour* in this case) provides the basis for the reference frame. The nominal post-flight Shuttle orbit accuracies are at the 90 m level (radially) and hence overwhelm the error budget for the SLA instrument. Therefore, an alternative orbit and attitude determination technique has been employed.

The Tracking and Data Relay Satellite System (TDRSS) is the primary tracking data source for the Shuttle and is what we used for operational orbit determination. Despite the quality of the two-way range and range-rate tracking data between the Shuttle Orbiter and TDRSS, knowledge of the position of the TDRS spacecraft is limited to 30-50 m and is thus the dominant error source for Shuttle orbit determination. This deficiency can be overcome by exploiting the independent and precise knowledge of the TOPEX/POSEIDON (T/P) satellite trajectory, as outlined by Marshall et al. (1995a; 1995b) and Rowlands et al. (1995). T/P is a joint U.S.-French satellite which employs a real aperture radar altimeter (RAR) to investigate the Earth's ocean topography (Wingham et al., 1994). A wealth of Satellite Laser Ranging (SLR) and Doppler Orbitography and Radio Positioning Integrated by Satellite (DORIS) tracking data, coupled with enhanced spacecraft modeling, yield T/P radial orbit errors of less than 3 cm root mean square (RMS), and less than 10 cm in total position (Marshall et al., 1995a; 1995b; Rowlands et al., 1995). T/P is also tracked using TDRSS. Therefore, the T/P trajectory, independently determined from SLR and DORIS data, can be used as a roving ground station for TDRS spacecraft orbit determination. This technique reduces the total TDRS orbit errors to less than 5 m.

The TDRS ephemeris can thus be held fixed and, in conjunction with enhanced spacecraft modeling techniques, the Shuttle's position can be computed. Simultaneously, measured quaternions from the Shuttle's star trackers (i.e., attitude information) can be ingested into the Goddard Space Flight Center's state-of-the-art orbit determination system, known as GEODYN (Marshall et al., 1995a; 1995b; Rowlands et al., 1995), to properly orient the Shuttle, and hence the SLA sensor. Given the precise knowledge of SLA's position and pointing that can be derived using the method just described (i.e. to better than 0.03° in all 3 axes), the ranging measurements from SLA can be reduced to yield a latitude, longitude, and the derived height of the altimeter's "bounce point" with an accuracy commensurate with the instrument's intrinsic vertical resolution (~ 1 m). The error budget associated with this geolocation process is

summarized in Table 1. As the SLA-01 data is further analyzed and processing techniques are refined, the errors listed in Table 1 can be expected to decrease. It is

Table 1. Preliminary Error Budget for SLA

Error Source	*Radial Error (m)*	*Horizontal Error at the Surface (m)*
Orbit	< 1.5	< 5
Attitude	< 3.0	< SLA footprint
Altimeter bias	~ 0.2	< 1.5

instructive, however, to observe that even preliminary SLA altimetric data provide better than 2 m accuracies, which is of higher quality than all but the most local-scale topographic maps presently available (Loughridge, 1986; Madsen et al., 1993). Figure 2 graphically illustrates the vertical error budget of the SLA instrument by comparing all ocean surface observations to a Mean Sea Surface ocean topographic model, corrected for Ocean Tides, derived from Topex/Poseidon measurements. The RMS levels of disagreement of ~ 2.8 m can be explained by a combination of residual pointing errors, sea surface wave structure, and other biases not accounted for in the analysis of SLA data thus far. What is important to note, however, is that 2.8 m RMS quality topographic data can also be obtained by SLA over land targets.

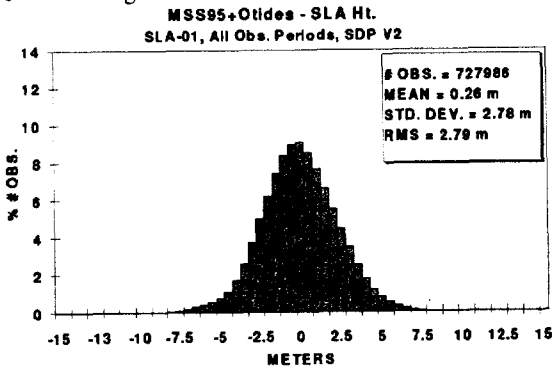

Fig. 2. Statistical comparison of SLA ranges to ocean surfaces with TOPEX-based Mean Sea Surface ocean topography corrected for ocean tides. Sea state effects have not been removed and are thus reflected in the 2.8 m RMS value.

5. SLA measurements and interpretations

During its almost 82 hours of operation during the January 1996 STS-72 Space Shuttle mission, the SLA instrument acquired ~ 3 million observations of the Earth's land, ocean, and cloud features. Robust ranging performance appears to be dependent, in part, upon solar illumination. False alarms were held at 1%, but the thresholds for triggering were raised to their maximum values by daytime solar reflection from clouds and thus some ranging data were lost. Late in the SLA observation sequence, for example, over 60% of the over land measurements made by the altimeter in a transect across South America resulted in a failure to achieve adequate detection signal-to-noise statistics (i.e., zero range indication). Such high levels of background were infrequently encountered, however, with the exception of localized, highly-vegetated portions of South America, central Africa, and Indonesia.

Data analysis of the 7 flight days of SLA operations (11 operational periods largely during crew sleep and rest periods) is complete and has required accurate (i.e., msec) time-merging of the SLA data stream with ancillary pointing and radial orbit information provided by NASA's Johnson Space Center Mission Evaluation Work Station or MEWS system. This has permitted us to georeference all SLA observations and to organize data acquisitions both by mission elapsed time (or UTC) and geographical position. Figure 1 illustrates the total ground-track coverage achieved during the STS-72 mission. Cloud-free land or ocean (water) surface measurements were obtained for ~54% of the Earth in the mid-latitudes. On the other hand, ranges apparently associated with discrete cloud features accounted for ~ 40% of the SLA observations, leaving ~ 5% to be explained by false alarms or missed pulses. For typical transcontinental transects in regions such as Africa, Asia, or Australia, as high as 95% of the attempted SLA observations resulted in reliable surface measurements, with the remaining few percent apparently associated with discrete cloud features. Cloud path lengths in such continental regions are typically less than 1 km, with cloud-to-cloud spacings of ~ 20 km. Thus, under favorable conditions, SLA achieved sub-kilometer horizontal sampling of the topography of continental-scale regions up to 5000 km in extent.

We have examined the preliminary ocean, land, and cloud coverage attained by SLA. Over 16.5% of the valid SLA observations (i.e., ~ 475,000) consist of land surface returns, while ~ 38% (i.e., ~ 1.1 million) represent ocean surface measurements. Figure 3 illustrates the distribution of surface and cloud-top returns achieved by SLA. We have separated the distribution of observed cloud-top heights into those measured over oceans versus those encountered over land surface targets. This allows us to address the vertical distribution of detectable cloud tops as a function of underlying surface topography. Statistically, cloud tops located 2.5 km above mean sea level occur more frequently over continental land masses than over oceans. Indeed, we have observed that cloud tops between 2.5 km and 7 km are two to four times more common over land than over oceans. However, cloud tops above about 7.5 km appear equally frequent over continental and ocean targets. Orographic effects appear to have influenced the cloud top heights over land surfaces, at least in terms of those types of clouds for which SLA reliably achieves valid ranges.

When SLA's ~ 344,000 precisely georeferenced land surface elevations are compared against the available global Earth Digital Elevation Models (DEM's), there is generally good agreement, although discrepancies are especially noticeable in areas with less than 100 m of relief. The distribution of ocean surface elevations achieved by SLA are cast in an ellipsoidal reference frame, so that ~ 100 m of relief variability observed in Fig. 3 is caused by variations in the geoid. Indeed, when SLA's ocean surface observations are compared against mean sea surface

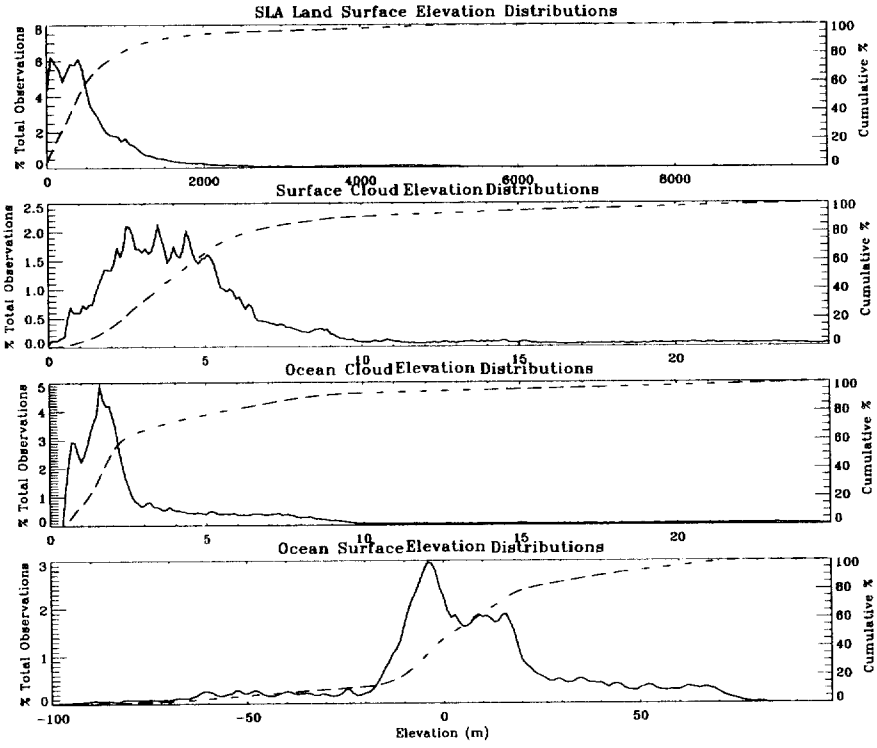

Fig. 3. Histograms of SLA measurements of land surface topography (top), cloud top heights over land, cloud top heights over oceans, and ocean surface elevations (bottom). All histograms are plotted in frequency (solid) and cumulative (dashed) formats.

models, corrected for tidal variations, as derived from the latest Topex/Poseidon measurements, RMS differences less than 2.8 m are observed (Fig. 2), with the suggestion that overall differences can be reduced to ~ 1.5 m with more refined processing of the SLA data.

Topographic studies of terrestrial land surfaces naturally fall into categories associated with important surfaces processes, including tectonism, erosion, volcanism, anthropogenic influences, ecosystems, and so-called "extremal events" or natural hazards. Furthermore, since almost all of the landscapes on Earth display some forms of vegetation, the dynamics of the vegetation cover associated with various classes of landscapes must also be considered. Thus, SLA's most direct contribution to studies of the global Earth system fall within the subdiscipline often referred to as "land cover" and its dynamics.

6. Observations of a Hawaiian volcano

In order to illustrate how the SLA system acquired some of its initial data (13 January 1996), an example is provided in Fig. 4. In this case, an SLA transect across the island of Hawaii is featured. The segment of data that is plotted is from the first orbit during which SLA was activated, and it extends from WNW to ESE across an expanse of the central Pacific Ocean, during which fortuitously the Shuttle *Endeavour*'s ground track passed over the near-summit region of a 4000 m composite shield volcano known as Mauna Kea, on the island of Hawaii. The cloud-free nature of the topography of the north-central island of Hawaii is evident in the data, as Mauna Kea looms as a 4000 m high feature in the SLA elevation dataset. Parasitic cinder cones on the WNW flank of this important volcano are observed (Fig. 4), as well as the classic break in slope that discriminates the lower shield (plinth) from the alkalic and more-explosive summit region. If one applies the methods described in Garvin (1996) to mathematically characterize the topology of Mauna Kea as measured by SLA, in contrast to that which would be modelled from a 90 m spatial resolution DEM (top of Fig. 4), there is agreement at the 10% level for the volume and surface area of the upper 2000 m of the edifice. Ranging reliability was nominal for the entire Mauna Kea transect. Figure 4 further illustrates the results of comparing preliminary SLA topographic data with a 90 m spatial resolution digital elevation model (DEM) for the Mauna Kea volcano (Moore and Mark, 1992).

After suitable correction of pointing errors associated with the apparent roll of the Shuttle Orbiter, a total error budget of 13 m RMS is computed. This cumulative error is mostly likely a consequence of the ~ 16 m intrinsic vertical precision of the reference DEM, in combination with the effects of vegetation cover on the eastern flank of the Mauna Kea volcano. Further corrections for the pointing of the Shuttle Orbiter on the basis of analyses of ocean ranging biases can be shown to reduce these errors to 11.5 m RMS. These results, however, suggest that the SLA sensor is capable of ~10 m class precision topographic measurements from a spaceborne perspective, even for complex, rugged targets such as a 4000 m volcanic edifice. Even before complete calibration by means of echo analysis, this simple example demonstrates that extremely

high vertical precision topographic observations are possible with SLA data.

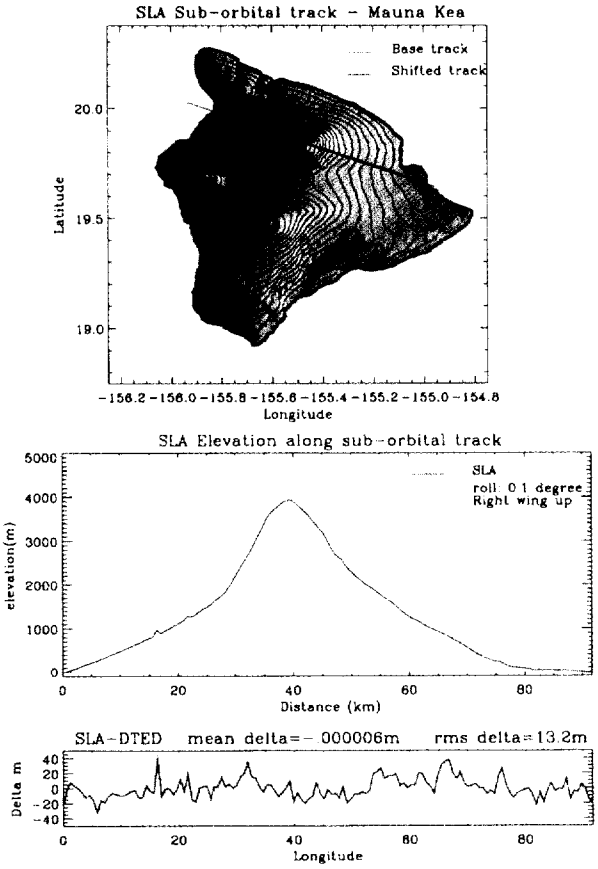

Fig. 4. SLA transect across Mauna Kea volcano illustrating its position on a shaded relief map of the island of Hawaii and the SLA transect achieved below. A total RMS difference between SLA's measurements and those from a 90 m spatial resolution DEM of ~ 13 m is observed, before final corrections for Shuttle attitude, which bring the RMS difference down to 11.5 m.

7. Observations of coastal deltas

SLA observations of coastal deltaic plains have also contributed new observations of the often mundane relief properties of these important landscapes. Figure 5 illustrates an SLA transect across the Irrawaddy deltaic plain of Burma. In this figure, the best available DEM for the region is shown in terms of shaded relief, with the SLA ground-track superimposed, and the SLA topographic cross-section is depicted as a profile of relief relative to mean sea level. In this case, the 7 to 35 m dynamic range of relative relief across a ~ 200 km wide region is evident from the SLA profile, while the 1 km DEM suggests a featureless plain. In the region between 94.5° E and 96.7° E longitude, the SLA ranging data suggest the intermittent detection of 7 to 30 m tall hills with superimposed trees, separated by essentially flat regions with less than 10 m of total relief. Given that SLA's surface footprint is 100 m in diameter and that the horizontal separation of its surface observations is ~ 700 m, the frequent detection of the apparent canopy tops of deltaic vegetation, provides new information on the spatial structure of vegetated deltaic plains in this region.

As can be observed in Fig. 5, the total dynamic range of ground elevations across the central portion of the Irrawaddy delta is < 20 m, with superimposed trees and hills between 7 m and 30 m in effective height as primary land cover. In the event of the typical surges of water triggered by tropical depressions in this region, a 3-4 m rise in the water level would essentially flood all of the unvegetated terrain within the entire delta, were it not for the vegetation. SLA recorded analogous information for other major coastal deltaic plains, including the Mekong, Indus, Ganges-Brahmaputra, and Senegal. In the distal portion of the Ganges delta , the dynamic range of ground relief is ~ 3 m across a 130 km wide expanse, with 6 - 20 m tall trees superimposed in isolated places, as in the Mekong. For the more arid Indus deltaic plain, the total dynamic range of observed topography is only 2-4 m, with no evidence of any superimposed arboreal vegetation. The relief observed by SLA for the wave-dominated Senegal delta in West Africa is similar to that measured for the Indus, perhaps on the basis of its aridity. Vegetated, humid

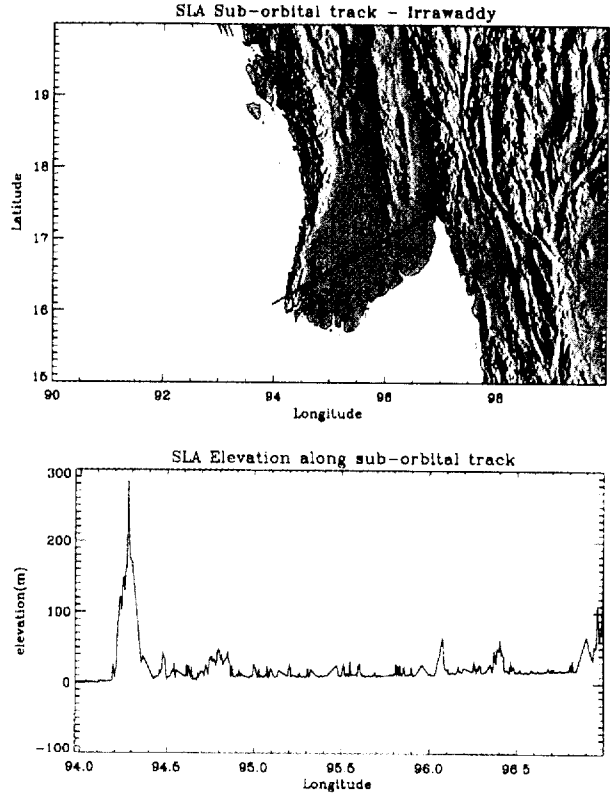

Fig. 5. SLA transect across Irrawaddy Delta showing ground track on shaded relief image and SLA topographic profile data below. Note the small amount of relief (< 30 m) between 94.5° and 96.8° E longitude.

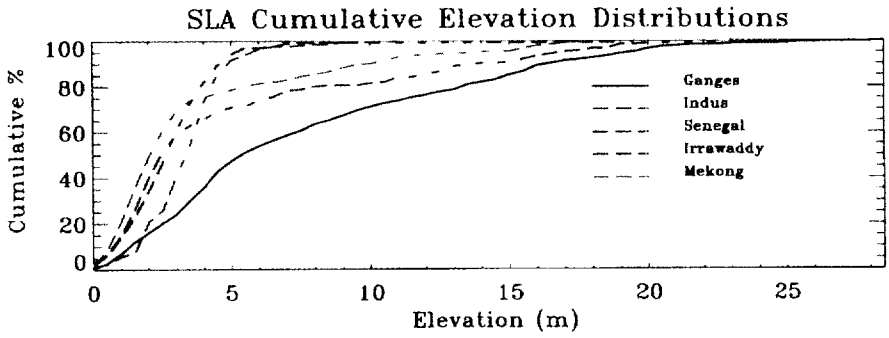

Fig. 6. Cumulative elevation (geoid-referenced) distributions for all SLA measurements of five major coastal deltaic plains. The arid deltas (Indus and Senegal) display different distributions than the humid varieties.

deltas such as the Ganges, Irrawaddy, and Mekong display distinctive cumulative distributions relative to arid deltas such as the Indus and Senegal. Over 90% of the local relief in the Indus and Senegal coastal deltaic plains is within 5 m of local sea level (Fig. 6). Storm-surge flooding of these arid deltas would thus be expected to completely inundate the deltaic surfaces, perhaps on an annual basis. Detecting and measuring the local heights of vegetation in coastal deltaic regions can be accomplished by context because of the extraordinarily benign local ground relief. Trees 9 to 20 m in relief are inferred from the SLA transects in the Ganges-Brahmaputra region, and such values agree with the best available published estimates (Coleman et al., 1989). However, direct detection of trees within individual SLA footprints by means of echo analysis can also be used to infer vegetation vertical structure under certain circumstances.

8. SLA echo analysis: background

As part of each SLA observation, a discrete "echo" or digitized waveform was acquired, an example of which from the coastal part of West Africa is illustrated in Fig. 7 . Such echoes are interestingly complex, and simple empirical correlations of first-order statistical descriptions of their shape properties (i.e., RMS pulsewidth, standard deviation of pulsewidth, total pulsewidth) with terrestrial surface types (i.e., land cover) has been undertaken for the entire dataset. In many cases, SLA echoes from minimally vegetated landscapes display distinctive characteristics suggesting that the uppermost or higher amplitude portions of such waveforms are truncated due to signal saturation. Slightly saturated echoes are frequently observed for land targets and this has plagued our derivation of unambiguous surface roughness properties in some cases. A significant fraction of those SLA echoes associated with vegetated surfaces display some degree of saturation (i.e. partial truncation of the highest amplitude portion). Comprehensive classification of all echo types and in-depth correlation of echo topologies with discrete surface types is presently underway. Here we discuss the first attempts at deriving a footprint-scale total vertical roughness estimate and, under some limited circumstances, tree canopy height information from echoes acquired by an orbital surface lidar.

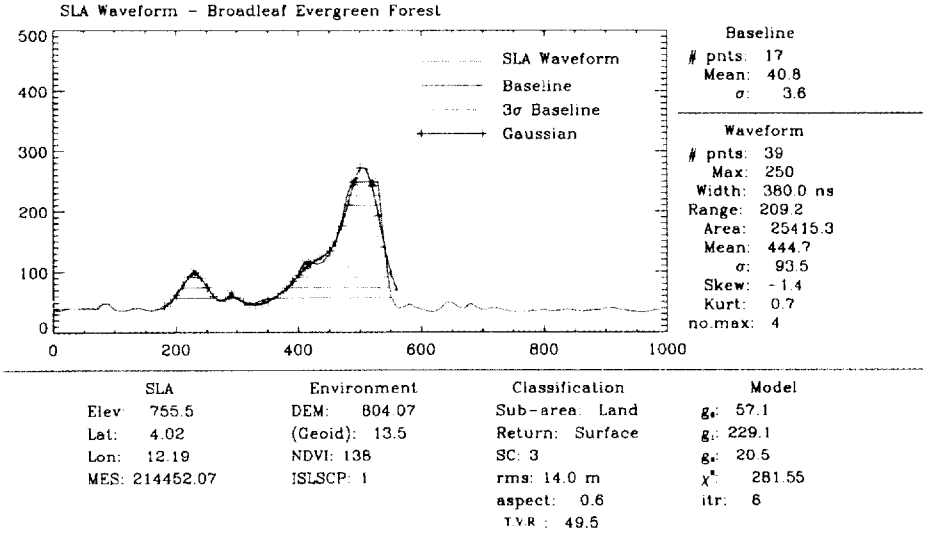

Fig. 7. Example of an SLA echo for a tropical forest surface in Cameroon, W. Africa, showing a clearly defined canopy vs. ground return (final large peak). Various statistical parameters are listed (see text).

For unvegetated, desert surfaces, SLA echoes vary from impulse-like, narrow-width varieties to highly dispersed types we believe to be associated with local topographic irregularities such as escarpments, gullies, yardangs, and dunes. Indeed, anywhere from 2 m to 60 m of effective total pulse spreading can be observed within 100 m diameter SLA footprints in unvegetated desert terrain. Complex, multi-modal echoes require special interpretation, but analysis of the total degree of pulse spreading, perhaps relative to that which is observed over ocean targets, provides a first-order estimate of a total vertical surface roughness parameter. Thus, 50 m total vertical roughness values, even within 100 m diameter surface footprints, are not unknown even in topographically benign parts of North Africa. The total vertical roughness is estimated on the basis of a multi-Gaussian parameterization of the echo. Bare, unvegetated desert surfaces in North Africa display total vertical roughnesses (5-15 m) that are sometimes little more than those most typical for ocean surfaces (i.e., ~1 - 3 m). In contrast, however, are echoes acquired by SLA for tropical forest regions. In many such cases, a bimodal SLA echo is observed in which a strong, Gaussian ground return is located nearly 100 ns (~ 15 m in range) after initial detection of a "surface" range (i.e., Fig. 7). This sort of bimodal behaviour has been extensively observed in aircraft laser altimeter datasets for forested surfaces (Harding et al., 1994b; Blair et al., 1994). Because SLA's footprints are substantially larger than the spatial scale of tree crowns, it is most likely that these sorts of echoes, of which there are many, provide a measurement of vegetation height for an assemblage of several trees in circumstances where the local ground slopes are less than a few degrees. From many examples where echoes are polymodal, it is possible to infer the Effective Canopy assemblage Height (ECH), a special form of total vertical roughness, as well as the vertical roughness of the ground beneath the canopy. However, without detailed ancillary information, perhaps as can be provided with 100 m or better resolution multispectral land imaging systems, it is difficult to isolate and interpret the individual vertical elements within SLA echoes, as can be accomplished with calibrated aircraft surface lidar data.

9. Measurements of vegetation

Empirical experience with remote tree height estimation has been amassed by scientists and engineers at NASA's Goddard Space Flight Center (Blair et al., 1994), using airborne surface lidar sensors (Harding et al., 1994b; Blair et al., 1994). However, airborne laser altimeter echo recovery algorithms produce optimal results for simultaneous estimation of the ground return and that of the canopy top when the scale of surface footprints matches the spatial pattern of the tree crowns being measured. From the experience gained by Blair, Harding, and colleagues (Harding et al., 1994b; Blair et al., 1994), optimal fooprints for robust estimation of tree heights for many vegetation surface types are typically 10 - 25 m in diameter, and certainly not as large as 100 m (i.e., the nominal SLA footprint diameter). Given this important proviso, effective canopy assemblage heights (ECH) have been extracted from SLA echoes only under those circumstances where the underlying ground relief is of low total variability and slowly varying (i.e., low local slopes), and where SLA echoes are not saturated.

Using algorithms for retrieval of tree heights from surface lidar echoes pioneered by Blair and others (Blair et al., 1994), the canopy top and underlying ground topography can be estimated exclusively using SLA echoes in areas of

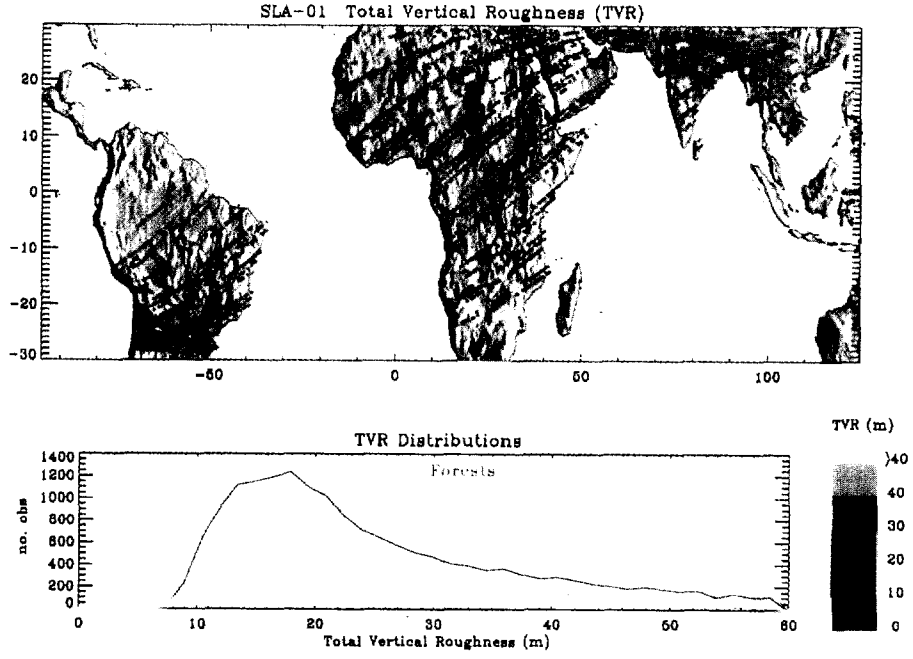

Fig. 8. Global map of SLA total vertical roughness (TVR) values superimposed on a shaded relief map of the Earth. The TVR values are color coded, and in regions of low slope, such values represent an estimated canopy assemblage height or ECH. Histograms of total vertical roughness for all vegetated land-cover classes versus that for arid lands are illustrated below. High TVR values in mountainous regions such as the Andes, Zagros, and in the Tibetan plateau reflect extreme local slopes and may not provide any information about the relief of vegetation, even if it is present. See text for details.

benign local topography. It appears that SLA's ability to quantify vegetation vertical structure is partially dependent on the local variability of the ground elevation, as well as upon the statistical character of the echoes. Well-behaved echoes associated with highly vegetated landscapes in Brazil, coastal Cameroon, the Congo Basin of Africa, and in Laos have been examined. It is apparent that improved algorithms for objectively isolating the ground return from that associated with a tree canopy top are needed if SLA echoes are to be used to dramatically extend the existing database of tree height observations. Many unsaturated SLA echoes have poorly expressed ground returns, perhaps due to local heterogeneities in vegetation cover (i.e., mixed target types). Furthermore, since SLA measurements consist of 100 m diameter footprints separated from their neighbors by at least 600 m, it is important to recognize that SLA's utility for vegetation parameter estimation is severely limited. Experience with aircraft echo recovery surface lidar systems by Blair, Harding, and colleagues (Harding et al., 1994b; Blair et al., 1994), indicate that contiguous sampling along track is required to consistently retrieve tree heights in their proper context, and to reliably estimate sub-canopy ground elevations and local slopes. Given these caveats, we have produced a best-efforts global assessment of effective canopy heights (ECH) using those SLA echoes suitable for this purpose (i.e., unsaturated, polymodal, strong final peak). A global map of the distribution of ECH (total vertical roughness) is presented in Fig. 8. In those cases where local slopes are high, we have computed a total vertical roughness (TVR) parameter using the same algorithm as for ECH, which is a representation of the maximum sensible variation in topography within a 100 m diameter SLA footprint. These values are plotted on Fig. 8 together with the ECH values for the purpose of demonstrating the global distribution of 100 m length scale vertical roughness. Thus, high ECH values in Iran and in central Asia represent steeply sloping, rugged terrain, and cannot be interpreted in terms of vegetation assemblage heights even in cases where trees are present.

10. Global roughness

The vertical structure of terrestrial landscapes at 100 m length scales is known for only a few well-studied field sites, such as the small patches of the boreal forest, the Kansas prairie, and localities within several tropical rainforests. If we compute a 100 m scale total vertical roughness parameter from the individual SLA echoes (i.e., as described above for ECH), and examine the correlation with local topography and regional land cover as measured from passive imaging in the visible and near-infrared, then one can assess empirically the scientific contribution such information would have on existing land-surface interaction models. We have taken the SLA echoes for all of the cloud-free land targets observed during the STS-72 mission, and have computed a total vertical roughness value for each echo where saturation is either non-existent or minimal. A global histogram of the frequency distribution of this total vertical roughness parameter (i.e., or ECH where vegetation is present) for all SLA land surface returns is featured in Fig. 9. For ocean surfaces adjacent to the land surface portion of this dataset, we have also estimated the vertical roughness, which varies from 1.2 to 3 m RMS. If we adjust the computed roughness values so that the roughness of ocean surfaces is zero to 2 m in order to compensate for the system delay and impulse response of the SLA sensor, then the frequency distribution of relative total vertical roughness over land targets varies from 2 to 55 m, with a corrected mean value of ~ 27 m. Local slopes at 100 m scales corresponding to such vertical roughness values range from 1.1° to 26°. Total vertical roughness values in excess of 20 m (after correction as above) can be observed to occur in areas of increased local topographic complexity, such as within large mountain zones (Zagros), in areas dominated by tropical forests, and when rift flank mountains are present. These areas make up only a few percent of the entire SLA dataset. It appears that most Saharan and Arabian deserts display total vertical roughness values in the 10 - 30 m range, with a most typical value of

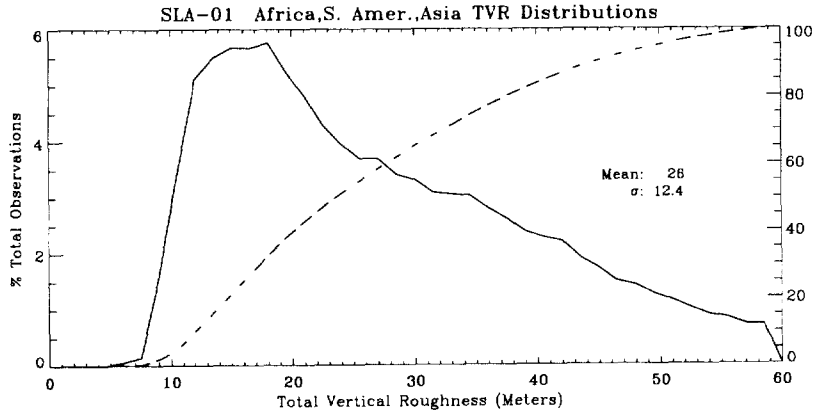

Fig. 9. Frequency and Cumulative distribution of total vertical roughness (ECH in cases of low slope) for all of the Earth's land areas sampled by SLA. The derivation of this parameter is only permitted in cases where the echoes are largely unsaturated and when they display a polymodal character (i.e., ~ 20% of the land surface measurements achieved). See text for details.

11- 20 m, corresponding to a within-footprint local slope of ~ 6.0°. This value is surprisingly similar to the many of the RMS slope values derived from quasispecular microwave scattering measurements for some parts of the expansive rolling plains of Venus, perhaps attesting to the similar local roughness of terrestrial deserts, at least at 100 m length scales. In addition, it appears that the 100-m scale total vertical roughness of such terrestrial deserts, as inferred from SLA echoes, is consistently similar to values derived from Earth-based radar scattering observations of Northern Hemisphere landing site regions on Mars (Harmon, 1997). MOLA-2 observations of RMS optical pulse width for the martian surface, as available in 1998, facilitate direct comparisons of terrestrial deserts (as measured by means of SLA echoes) with martian surfaces. Initial indications suggest that martian northern plains surfaces are slightly smoother at 100-200 m length scales than the subset of terrestrial deserts sampled by SLA (Smith et al., 1998).

11. Correlations with land cover classes

One can extend this SLA echo analysis to regions dominated by more complex land cover patterns, including widespread vegetation. We have taken an SLA transect that crosses at least six global land cover classes between tropical forests in West Africa (Cameroon) to the mixed woodlands and savannahs of Sudan, and including bare sandy and stone pavement deserts, grasslands, and shrublands. In this case, we compute total vertical roughnesses for complex multimodal SLA echoes in all cases where only simple forms of saturation are observed; where multiple parts of an echo are saturated, it is impossible to unambiguously reconstruct the unsaturated echo shape, and no values are derived in such instances. Figure 10 illustrates the SLA transect in question both in terms of SLA-derived surface elevations and total vertical roughness, plotted as ECH. The frequency distribution of total vertical roughness (or ECH) is appreciably different in

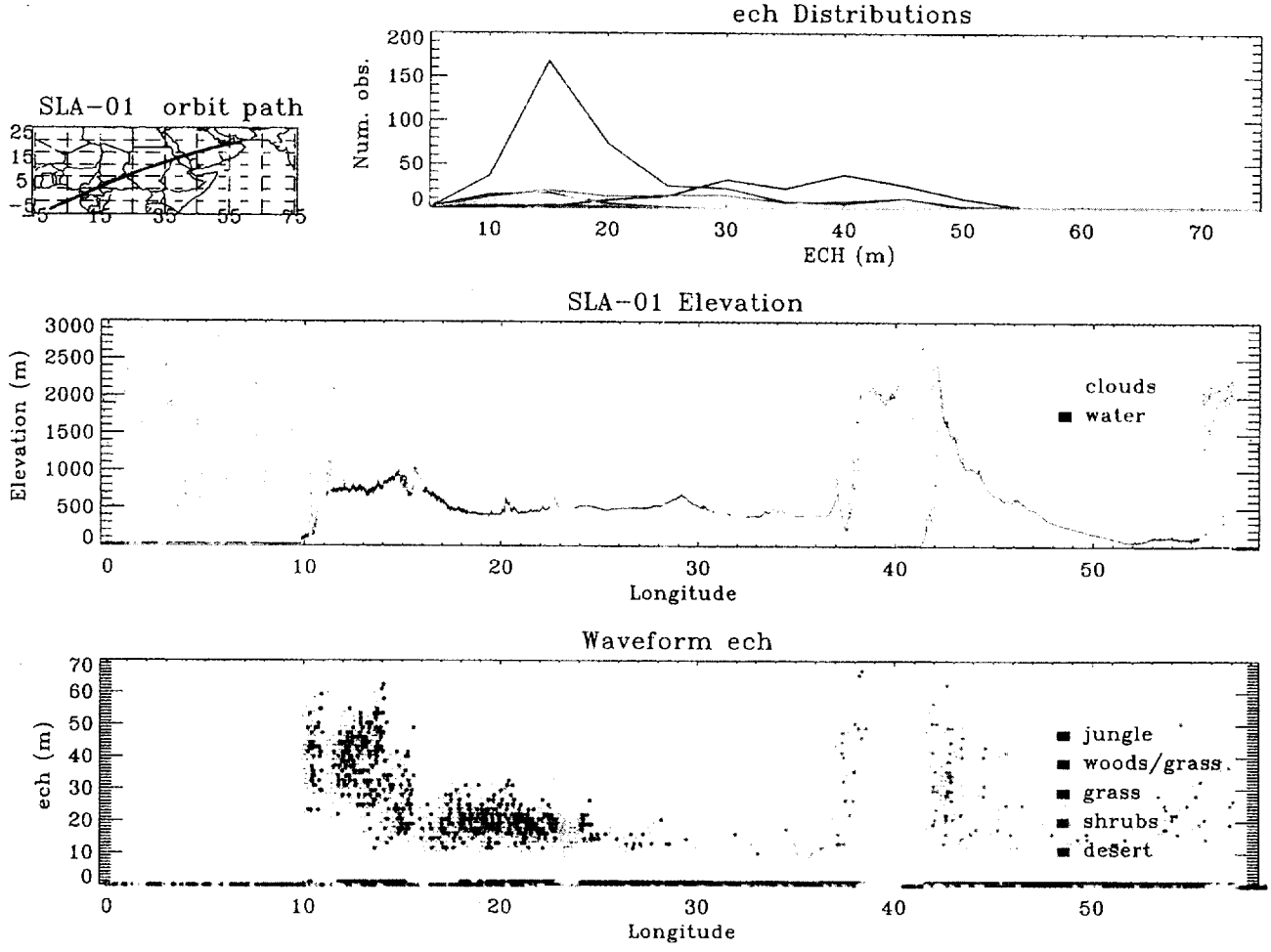

Fig. 10. Example of an SLA transect across central Africa illustrating the distribution of total vertical roughness derived from SLA echoes as in Fig. 8. In this case, the ECH roughness values corresponding to global land cover classes are plotted separately in the histogram in the upper right. Tropical forests display the widest range of ECH values, extending from 10 m to ~ 60 m, relative to ocean values.

this case than that for unvegetated North African deserts. In this more complex situation, total vertical roughness values for ocean and inland sea (water) surfaces vary from 1.2 to 3 m, with a modal value of 1.5 m. If we assume, as before, that the ocean surface vertical roughness includes the effect of the SLA instrument impulse response, and translate the computed values so that the modal ocean surface has a 0-1 m total vertical roughness, then the frequency distribution of central African land surface vertical roughness varies from less than 5 m (deserts) to 60 m (tropical forest landscapes). Such values correspond to local slopes at 100 m length scales that range from 2.8° to 31°, with a modal value of 8.5°. The important difference here (Fig. 10) is that we have subdivided the frequency distribution of total vertical roughness values as a function of the land cover types to which they belong, using the color conventions illustrated in the lowermost profile. Tropical forest surfaces ("jungle" in the lowermost panel of Fig. 10) display corrected total vertical roughness values (ECH) that vary from 10 m to 60 m, suggesting that SLA echoes are at least indirectly recovering some aspects of the vertical structure of the local forest cover. We recognize that a more refined estimator for vegetation canopy height must be developed, but our experiment with a simple statistical estimate of within-footprint vertical roughness indicates that global land cover classes have distinctive signatures in terms of their SLA-derived roughness values. Tropical forests in western Africa (Cameroon) display total vertical roughness values that vary from 7 m to nearly 60 m, while Sudanese grasslands display values most similar to those for stony deserts. Were it not for echo saturation effects which restrict the number of valid SLA measurements, the correlation of total vertical roughness statistics with land cover classification would allow for discrimination of global land cover classes solely on the basis of SLA echo properties.

12. Ocean surface observations.

Observations of the global ocean surface with SLA is yet another element of our investigation of the Earth using the perspective provided by orbital surface lidar. Even before including high precision radial orbit information and attitude data, SLA ranging data over oceans can be used to demonstrate the reliability of the instrument's ranging performance. For example, a ~ 200 km segment of detrended SLA data across the Red Sea indicates a total dynamic range of relief of ~ 4 m, with a standard deviation of 0.9 m. In a ~ 1000 km stretch of Pacific Ocean east of Hawaii (i.e., between 144° and 154° E longitude), a similar statistical trend was observed, with a standard deviation of 0.9 m, and a total dynamic range of ~ 5 m. Thus, we are confident that SLA has produced meter-quality elevation measurements of both land and oceanic surfaces with an orbital laser altimeter system. When precision orbits and attitude information are utilized (Rowlands et al., 1997), the difference between SLA's observations of ocean surfaces and those measured by the Topex/Poseidon ocean radar altimeter in terms of a mean sea surface are smaller than 2.8 m RMS. By more fully correcting for additional aspects of Shuttle attitude and platform motion uncertainties, we have indications that 1.7 m RMS quality data can be achieved for ocean surface targets.

13. General land observations

Over land, RMS discrepancies between SLA and the best available 90 m and 1000 m spatial resolution DEM's range from 2-5 m in low-lying coastal regions to 12 m RMS over volcanoes such as Mauna Kea, and are as high as 50 m in complex unvegetated regions, such as the Zagros Mountains of Iran. We have intercompared all 32 SLA transects over Africa for which high precision orbits are available against the best available 1 km spatial resolution DEM for this region. The standard deviations of the differences between SLA's ellipsoidally-referenced surface elevation measurements and those reported in the 1 km DEM vary from ~ 40 m in the North African desert regions to 150 m in the tropical forests of central Africa. SLA echoes for heavily vegetated parts of Africa (i.e., on the basis of global land cover models) suggest total vertical roughness values over 50 m, which may be correlated with vegetation canopies that are as tall as 40-60 m. Since existing DEM's do not systematically record "bare-earth" surface elevation values, some of the discrepancies between SLA measurements and these DEM's may be due to vegetation vertical structure. Within Africa, where the source of the DEM data is digitized contour maps, discrepancies between SLA and such DEM's are often as high as 100's of meters, suggesting that many existing maps (and DEM's) are woefully inadequate in such regions as a source of topographic ground control points. We recognize, however, on the basis of SLA echoes, that up to perhaps 30 m of bias may exist in SLA's reported observations of surface elevations, because we have not yet included range-walk, amplitude, and centroid corrections into our computations of range. In cases where we have compared SLA to DEM's for coastal deltaic plains, we have converted SLA ellipsoidally-referenced elevations into orthometric (i.e., geoid-corrected) heights so that they locally approximate mean sea level. Even in such cases, differences by as much as 10-25 m are observed (i.e., in the distal Ganges), suggesting that existing DEM's may not accurately reflect the current character of local relief variations in such highly dynamic regions.

SLA's land surface elevation and echoes dataset consists of almost an order of magnitude more observations (~450,000) than any previous spaceborne laser altimeter dataset (i.e., Clementine for the Moon). Each of SLA's land surface measurements have an intrinsic meter-level of vertical uncertainty, and when combined with the highest precision orbit and attitude data that is presently available, these data can be used to address issues associated with changing land cover patterns for many of Earth's continental regions at sub-kilometer length scales with very high vertical resolution. We have endeavored to make

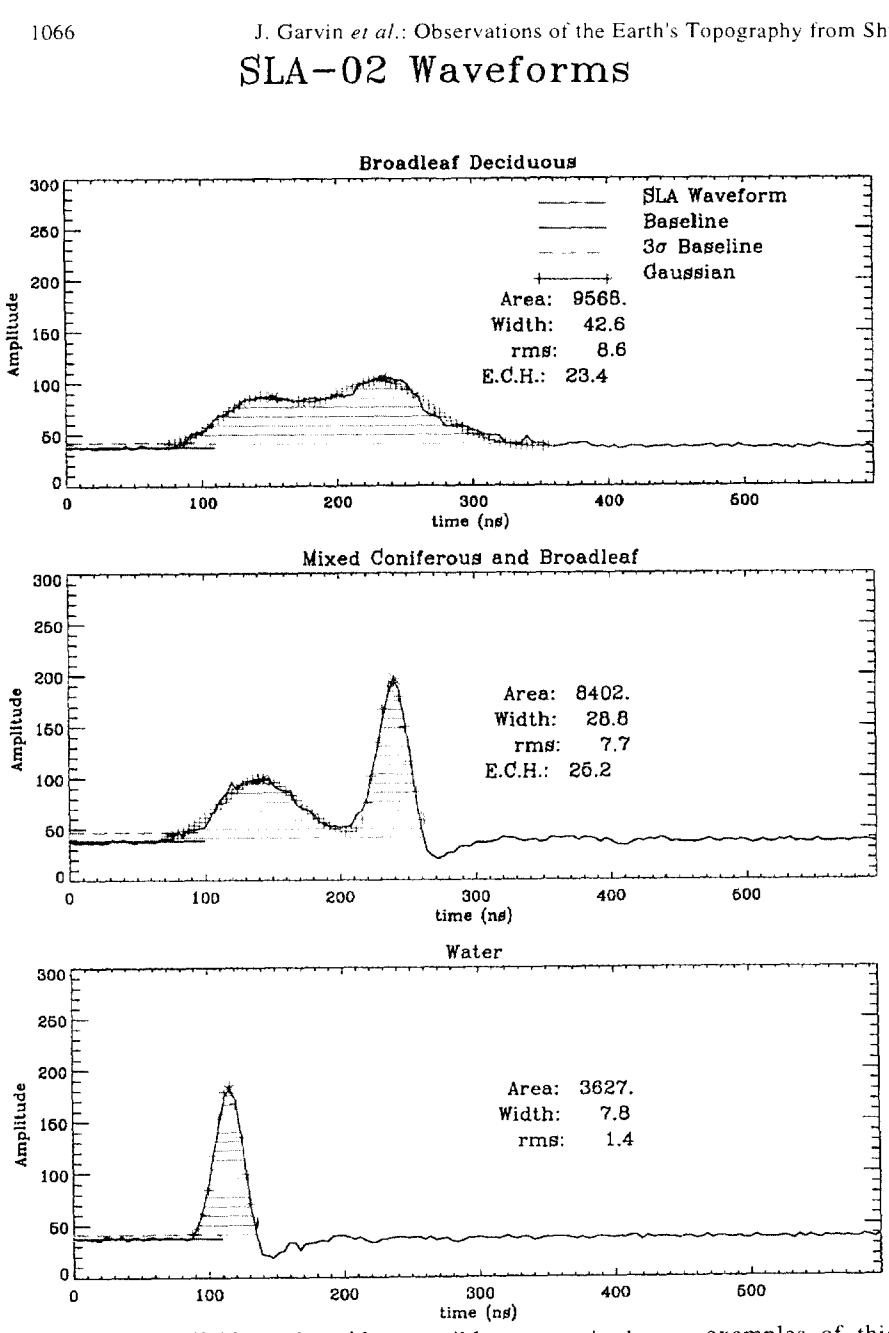

Fig. 11. Example SLA-02 echoes from Eastern United States for end-member land-cover classes. See text for details. RMS pulse width in meters and effective canopy assemblage height (ECH) values are listed.

these data available to the widest possible community by advertizing the best of the SLA-01 experiment dataset at a public web site (http://denali.gsfcnasa.gov/SLA). Very recently, a second spaceflight of SLA was successfully achieved as part of the STS-85 mission on the Space Shuttle *Discovery*. In this case, a variable gain state amplifier (VGA) was included within the SLA altimeter electronics to minimize echo saturation and this modification proved effective. Although these data have not been fully reduced, over one million unsaturated orbital surface lidar echoes were acquired by the SLA-02 experiment during its August 1997 spaceflight. Figure 11 illustrates three varieties for target areas in the Eastern United States, including conifers in New York state with clear definition of a strong ground return (i.e., middle echo in Fig. 11). These data will be made available in 1998, and the SLA-02 website illustrates examples of this new dataset (http://denali.gsfc.nasa.gov/sla02). Beyond SLA-02, plans for additional flights of embellished Shuttle Laser Altimeter sensors as early as late 1999 are under development, with higher pulse repetition rate (> 100 Hz) operations and smaller surface footprints among the objectives. NASA is presently supporting the development of an advanced multibeam laser altimeter satellite, known as the Vegetation Canopy Lidar (VCL), as part of its Earth System Science Pathfinder program, for spaceflight in 2000. In addition, as part of the NASA Earth Observing System, a high vertical accuracy laser altimeter and atmospheric lidar sensor (GLAS: Geoscience Laser Altimeter System) will be flown in polar orbit in mid-2001. These future systems (VCL, GLAS) have benefited from the results of the SLA-01 experiment.

14. Summary

SLA's maiden spaceflight successfully demonstrated a new class of technology capable of extremely precise topographic measurements of landscapes, ocean surfaces, and cloud-tops from a spaceborne perspective. As such, SLA has effectively validated the first generation of technologies that are required for long-term orbital monitoring of the mass-balance of the great polar ice sheets (Antarctica and Greenland) (Burke and Dixon, 1988; TOPSAT Working Group, 1994; Cohen et al., 1987). In addition, SLA observations have demonstrated a new form of topographic remote sensing that permits direct detection and measurement of the relief characteristics of mundane coastal landscapes, ephemeral desert landforms, complex mountainous terrain, and heavily forested surfaces. Furthermore, SLA's echoes can be used, under appropriate circumstances, to measure the heights of forest canopies in areas of low relief and slope, as well as the vertical roughness of desert surfaces (Garvin et al., 1998). Finally, SLA's observations of the spatial and vertical patterns of clouds within the mid-latitudes of the Earth in northern hemisphere winter conditions indicate that typical cloud cover is intermittent, with mean cloud path lengths of ~ 4 km, and a total percentage of quasi-global cloud cover of 40-45 %. This is encouraging in that it validates global cloud cover prediction models (Harding et al., 1994a) which suggest that on the order of 50% of the Earth's surface is cloud obscured during winter conditions. The vertical character of the Earth's land and ocean surfaces at 100 m spatial scales does not appear to inhibit the ability of orbital laser altimeter sensors such as SLA from precisely determining local surface elevations. Finally, the largest number of ground elevation observations afforded by SLA's initial spaceflight are in Africa, where the quality of existing DEM's is commonly questionable at levels of 100 m to 1000 m in a vertical sense (Burke and Dixon, 1988; Loughridge, 1986). Thus, the ~ 200,000 valid ground observations in Africa provided by SLA can be used by others to refine existing DEM's for this major continent, thereby improving an important foundation dataset for use by Earth scientists and others interested in modelling global patterns of surface change.

Acknowledgements. We wish to acknowledge the essential efforts of David Rabine and John Cavanaugh in this work. In addition, the outstanding support of the entire SLA engineering team is greatly appreciated. The Hitchhiker payload support staff, under the leadership of T. Dixon and A. J. Alfonzo, was instrumental to the successful acquisition of SLA data during STS-72. We are further grateful to the crew of STS-72 who kindly supported our observations during their very busy flight. Office of Earth Science Flight director R. Price kindly funded our SLA efforts, after the NASA Goddard Space Flight Center Director's Discretionary Fund provided the essential start-up support (courtesy Dr. Rothenberg, Center Director and Gerry Soffen). Special thanks to D. E. Smith (Principal Investigator, MOLA) for providing flight spare components to the SLA team. Additional thanks to Jim Roark, D. Barry Coyle, Dan Hopf, and Nita Walsh, who kindly spent many long hours in the POCC during the time in which SLA was collecting data. Finally, special thanks to Richard S. Williams Jr. (USGS), Tim Mutch (deceased), and Dr. Noel Hinners (Lockheed Martin) for their motivation of this effort over many years. JBG was strongly supported in his efforts with SLA by his wife Cindy, son Zack, daughter Danica, and Bouvier *Georgie-girl*. Many additional engineers at NASA/GSFC assisted with the SLA development and spaceflight, and we thank them for their much-appreciated efforts. SLA-02 conducted its spaceflight aboard *Discovery* on the STS-85 mission in Aug. 1997 in a 57° orbit. We gratefully acknowledge ongoing NASA support under RTOPs : 618-90-03, 622-19-15 (JBG), and 334-36-10 (PIDDP).

References

Balin, Y. et al., Joint interpretation of lidar and photometric data in the spaceborne measurements of cloud fields, *Proceedings of SPIE, vol. 2310*, 160 (1994).

Bindschadler, R. A. et al., Surface topography of the Greenland ice sheet from satellite radar altimetry, *NASA SP-503* (1989).

Blair, J. B., Coyle, D. B., Bufton, J. L., and Harding, D. J., Optimization of an airborne laser altimeter for remote sensing of vegetation and tree canopies, *Proc. Intl. Geosci. and Remote Sensing Symp. 1994, Vol. II*, 939-942 (1994).

Bufton, J. L., *Proc. IEEE, Vol. 77*, 463 (1989).

Bufton, J. L. et al., *Optical Engineering, Vol. 30 (1)*, 72 (1991).

Bufton, J. L., Blair, J. B., Cavanaugh, J., Garvin, J. B., Harding, D., Hopf, D., Kirks, K., Rabine, D., and Walsh, N., *Proc. 1995 Shuttle Small Payloads Symposium, NASA CR-3310* (1995), p. 83-91; Bufton, J. L. and Blair, J. B., "Space Laser Altimetry...", *The Review of Laser Engineering, Vol. 24 (12)*, 1285 (1996).

Burke, K. and Dixon, T., *NASA Topographic Science Working Group Report*,Lunar and Planetary Institute, Houston, Texas (1988).

Chao, B. F. and Naito, I., *EOS Trans. Amer. Geophys. Union, Vol. 76 (16)*, 164 (1995).

Cohen, S. C. et al., The Geoscience Laser Altimetry/Ranging System, *IEEE Trans. Geosci. Rem. Sens., GE-25*, 581 (1987).

Coleman, J. M, Roberts, H., and Huh, O. K., in *Geomorphology from Space*, Short, N., and Blair, R. (eds.), *NASA SP-426*, Washington, DC (1989), pp. 317-340.

Coleman, J. M and Wright, L. D., "Modern River Deltas: Variability of Process and Sand Bodies", in M. L. Broussard (ed.) *Deltas: Models for Exploration*, Houston Geological Society Publication, 1975, pp. 99-149.

Evans, D. L. et al., *EOS Trans. Amer. Geophys. Union, Vol. 75 (52)*, 553 (1992).

Gardner, C. S., *IEEE Trans. Geosci. Rem. Sens., Vol. 30*, 1061 (1992).

Garvin, J. B., *Photonics Spectra, Vol. 37*, 67 (1993).

Garvin, J. B., *Geol. Soc. London Special Public. 110*, 137 (1996); in McGuire, W., Jones, A., and Neuberg, J. (eds) *Volcano Instability on the Earth and Planets, Geol. Soc. Spec. Pub. 110.*

Garvin, J. B., Blair, J. B., Bufton, J. L., and Harding, D. J., *EOS Trans. AGU, Vol. 77 (7)*, 239 (1996a)

Garvin, J. B., Harding, D. J., Blair, J. B., Frawley, J. J., *EOS Trans. AGU, Vol. 77 (46)*, F32 (1996b).

Garvin, J. B., "Coastal Hazards Monitoring and Topographic Characterization by means of Laser Altimetry", in *Proceedings of Coastal Hazards Workshop, Louisiana State University, Coastal Studies Institute Publication*, editted by Huh, O., LSU Technical Report TR-654, 39 (1997).

Garvin, J. B. et al., Three Dimensional Structure of Terrestrial Landcover and Landscapes as Determined by Shuttle Laser Altimeter (SLA) Observations, submitted to *Nature*, 15 pp (1998).

Harding, D. J., Bufton, J. L., and Frawley, J. J., *IEEE Trans. Geosci. Rem. Sens., Vol. 32 (2)*, 329 (1994).

Harding, D. J., Blair, J. B., and Garvin, J. B., Laser altimetry waveform measurement of vegetation canopy structure, *Proc. Intl. Geosci. and Remote Sensing Symp. 1994, Vol. II*, 1251-1253 (1994).

Harmon, J. K., *J. Geophys. Res., Vol. 102 (E2)*, 4081 (1997).

Krabill, W. et al., *Geophys. Res. Letters, Vol. 22 (17)*, 2341 (1995).

Krabill, W. et al., *Int. J. Remote Sensing, Vol. 16 (7)*, 1211 (1995).

Lancaster, N., *Geomorphology of Desert Dunes*, (Routledge, New York, 1995).

Loughridge, M. S., *EOS Trans. Amer. Geophys. Union, Vol. 67*, 121 (1986).

Madsen, S. N., Zebker, H. A., and Martin, J., Topographic Mapping using Radar Interferometry: Processing Techniques, *IEEE Trans. on Geosci. and Rem. Sens., 31 (1)*, 246 (1993).

Marshall, J. A., Lemoine, F. G., Luthcke, S. B., Chan, J. C., Cox, C. M., Rowton, S. C., Williamson, R. G., Wiser, J. L., *Paper IAF-95-A.1.05 at the 46th International Astronautical Congress, Oct. 1995*, Oslo, Norway (1995a)

Marshall, J. A., Zelensky, N. P., Luthcke, S. B., Rachlin, K. E, Williamson, R. G., *J. Geophys. Res. 100 (C12)*, 25331 (1995b)

Matvienko, G. et al., Spaceborne lidar for cloud monitoring, *Proc. SPIE, Vol. 2310*, 129 (1994).

Matvienko, G. et al., Space laser rangefinder "LORA" used as a cloud lidar, *Optical Review, Vol. 2*, 221 (1995).

Moore, J. G. and Mark, R. K., *GSA Today, Vol. 2 (12)*, 257 (1992).

Mouginis-Mark, P. J. and Garbeil, H., *Bulletin of Volcanology, Vol. 55*, 566 (1993).
Rowlands, D. D., Marshall, J. A., Pavlis, D. E., Moore, D., Rowton, S. C., Lou, S, McCarthy, J. J., Luthcke, S. B., *GEODYN II System Description*, Hughes STX Contractor Report, Greenbelt, MD (1995).
Rowlands, D. D. et al., Space Shuttle Precision Orbit Determination in Support of SLA-01 using TDRSS and GPS Tracking Data, *Journal of Astronautical Sciences, Vol. 46, No. 1*, 113 (1997).
Smith, D. E. et al., Topography of the Moon from the Clementine LIDAR, *J. Geophys. Research, Vol. 102 (E1)*, 1591 (1997).
Smith, D. E. et al., Topography of the Northern Hemisphere of Mars from the Mars Orbiter Laser Altimeter, in press in *Science* (1998)
TOPSAT Working Group, Scientific Requirements of a Future Space Global Topography Mission, *Italian Space Agency (ASI) Report ASI-92-RS-52*, 85 pp. (1994).
Wingham, D. J., Rapley, C., and Morley, J. G., *EOS Trans. Amer. Geophys. Union, Vol. 74 (10)*, 113 (1993); Fu, L. L., Christensen, E. J, Yamarone, C. A., Lefebvre, M., Menard, Y., Dorrer, M., Escudier, P., *J. Geophys. Res. 99 (C12)*, 24369 (1994).
Winker, D. M., Couch, R. H., and McCormick, M. P., *Proc. IEEE, Vol. 84 (2)*, 164 (1996).
Wright, L. D., "River Deltas", in *Coastal Sedimentary Environments*, Davis, R. A. (editor), pp. 1-76 (Springer, New York, 1985).
Zebker, H. A. et al., *IEEE Trans. Geosci. and Rem. Sens., Vol. 30*, 933 (1992).
Zebker, H. A. et al., *J. Geophys. Res., Vol. 99 (B10)*, 19617 (1994).
Zwally, H. J. et al., Surface Elevation Contours of Greenland and Antarctic Ice Sheets, *J. Geophys. Res., 88 (C3)*, 1589(1983).
Zuber, M. T. et al., *J. Geophys. Res. 97 (E5)*, 7781 (1992).
Zuber, M. T. et al., *Science, Vol. 266*, 1839 (1994).